Available online at www.sciencedirect.com
ScienceDirect
Journal of Power Sources 167 (2007) 330–335
JOURNAL OF POWER SOURCES
www.elsevier.com/locate/jpowsour

Short communication

Carbon nano-chain and carbon nano-fibers based gas diffusion layers for proton exchange membrane fuel cells

Arunachala M. Kannan *, Lakshmi Munukutla

Electronic Systems Department, 7001 E Williams Field Road, Arizona State University at the Polytechnic campus, Mesa, AZ 85212, USA

Received 16 December 2006; received in revised form 1 February 2007; accepted 2 February 2007
Available online 3 March 2007

Abstract

Gas diffusion layers (GDL) for proton exchange membrane fuel cell have been developed using a partially ordered graphitized nano-carbon chain (Pureblack® carbon) and carbon nano-fibers. The GDL samples' characteristics such as, surface morphology, surface energy, bubble-point pressure and pore size distribution were characterized using electron microscope, inverse gas chromatograph, gas permeability and mercury porosimetry, respectively. Fuel cell performance of the GDLs was evaluated using single cell with hydrogen/air at ambient pressure, 70 °C and 100% RH. The GDLs with combination of vapor grown carbon nano-fibers with Pureblack carbon showed significant improvement in mechanical robustness as well as fuel cell performance. The micro-porous layer of the GDLs as seen under scanning electron microscope showed excellent surface morphology showing the reinforcement with nano-fibers and the surface homogeneity without any cracks.

Keywords: Gas diffusion layers; Pureblack® carbon; Carbon nano-fibers; Inverse gas chromatography; Surface energy

1. Introduction

Proton exchange membrane fuel cells (PEMFCs) are attracting considerable interest as alternative power sources for automotive, stationary and portable applications due to their higher power densities and environmental benefits. However, when air is used as oxidant the power density values are reduced due to mass transport limitations primarily at the cathode. GDL is one of the critical components of a fuel cell that has the ability to influence the H_2/air system performance at high current density region. The water retaining (hydrophilicity) and water expelling (hydrophobicity) properties of the GDLs have to be carefully balanced to achieve optimal performance of the fuel cell without flooding when it operates under the condition of 100% RH [1–4]. The hydrophilicity of the gas diffusion layers can also avoid drying of electrolyte in lower RH conditions [5]. The essential functions of gas diffusion layers in a fuel cell are: distribution of reactants to the active site of electrode (pore size as well as porosity distribution), management of water supplied and/or generated and enhancement of electrical contact between the electrode and the bipolar plates [6,7].

Hence, the ideal GDLs should have good gas diffusion properties with optimum bending stiffness, air permeability, surface contact angle, porosity, water vapor diffusion, good electrical/electronic conductivity, crack free surface morphology, high mechanical integrity and enhanced oxidative stability along durability at various operating conditions including freezing condition [8–14]. The literature also deals with characterizing the GDLs and more specifically, methods developed for estimating the transport properties of GDLs are being published by Zawodzinski's group at the Case Western Reserve University along with E-Tek [15,16]. Recently, Wang et al. [17,18] reported a composite micro-porous layer in the GDL for improving the gas diffusion characteristics through the introduction of bi-functional pore structure. More recently, Kannan et al. has reported the use of Pureblack® carbon as a better material for the fabrication of micro-porous layer for gas diffusion layer compared to Vulcan-XC72R [19,20]. The objective of this study was to circumvent the mass transport limitation by designing an optimized membrane electrode assembly (MEA) configuration using nano-carbon chain (Pureblack) and nano-fibers based gas diffusion layers (GDLs). The properties of gas diffusion layers were appraised using scanning electron microscope

* Corresponding author. Tel.: +1 480 727 1102; fax: +1 480 727 1723.
E-mail address: amk@asu.edu (A.M. Kannan).

0378-7753/$ – see front matter © 2007 Elsevier B.V. All rights reserved.
doi:10.1016/j.jpowsour.2007.02.064

(surface morphology), Hg porosimetry measurement (mean free pore size), permeability (bubble-point pressure), inverse gas chromatography (surface energy) and electrochemical testing at 70 °C.

2. Experimental

Gas diffusion layers were fabricated with teflonized non-woven carbon paper (P50T, Ballard Applied Materials) as a substrate. Hydrophobic characteristic of the micro-porous layers was provided by TE5839 Teflon suspension (Dupont). Nano-fibrous type carbon (VGCF-H available from Showa Denko America Inc., New York) was mixed with nano-chain Pureblack® 205-110 Carbon (available from Superior Graphite Co., Chicago, IL, USA) to provide improved mechanical strength and adhesion of the micro-porous layer with the macro-porous layer. In order to fabricate the micro-porous layers, slurry of carbons (50–50 wt.%) with PTFE dispersion in a mixture of isopropanol and de-ionized water mixture (80–20 volume ratio) was prepared by ultrasonication followed by magnetic stirring [20]. The control group GDLs were fabricated with a well known Vulcan XC-72R in a similar procedure. The slurry was applied on the carbon paper by micro-spraying technique. Subsequently, carbon paper with micro-porous layer was heat treated by sintering at 350 °C in air for about an hour. The carbon loading for the micro-porous layer was approximately 3 mg cm^{-2} and the PTFE content was 30 wt.%.

The surface morphology of the GDL samples was examined by JEOL JSM-5900LV scanning electron microscope. The robustness of the micro-porous layer and the adhesion of the micro-porous layer to the macro-porous substrate were evaluated by subjecting the GDLs to ultrasonic vibration.

Surface energy measurements were carried out (Surface Measurement Systems Inc., Allentown, PA) by inverse gas chromatography (IGC). IGC is a gas phase technique using pulses of solvent vapor (heptane, octane, nonane, and decane) as adsorptive component to probe the surface and bulk properties of particulate and fibrous materials [21–23]. A carrier gas (He) is used to transport the probe molecule (adsorptive) to the GDL samples (adsorbent). The GDL is placed into a column while a known adsorptive is used in the gas phase. Similar to analytical gas chromatography, the retention time is measured as the fundamental parameter and then converted into a retention volume, which is directly related to several physico-chemical properties of the GDLs (absorbent). For each sample, an IGC column was prepared by packing the sample into a standard column (300 mm long and 4 mm inner diameter). All columns were analyzed two times sequentially to check for irreversible chemisorption effects and equilibrium after preconditioning. Initially, the columns were pre-treated for 2 h at 30 °C and 0% RH in a helium carrier gas to condition the sample and remove sorbed water or residual solvents. Then, the surface energy measurements were performed at 0% RH (two times sequentially with a 2-h conditioning between runs). All experiments were carried out at 30 °C, 10 sccm total flow rate, and injection vapor concentration of 0.03 P/P_0 for all elutants using flame ionization detector (FID).

The specific surface energy (γ_S^{SP}) of the GDLs is calculated from the geometric mean of the γ_S^+ and γ_S^- values (the electron acceptor and donor parameters of the surface, respectively)

$$\gamma_S^{SP} = 2(\gamma_S^+ \cdot \gamma_S^-)^{1/2}$$

The total surface energy is calculated by adding the specific and dispersive contributions: $\gamma_S^T = \gamma_S^{SP} + \gamma_S^D$. Recently surface energy data for GDLs with various amounts of hydrophobic contents measured using Kruss Processor Tensiometer is reported by Gurau et al. as one of the valuable ex situ tools [16].

Mean flow pore size data were collected (Hollingsworth & Vose, West Groton, MA) by Permeability measurements using air [24]. The threshold pressure was also measured using bubble-point pressure method and this method is the most widely used for pore size determination. The underlining scientific principle of this technique is as follows: for a given fluid and pore size with a constant wetting, the pressure required to force an air bubble through the pore is inversely proportional to the size of the pore. The procedure for bubble-point measurement is described below. The top of the GDL is placed in contact with the liquid (water) the bottom with air, the GDL holder is connected to a source of a regulated pressure. The air pressure is gradually increased and the formation of bubbles on the liquid side is noted. At pressures below the bubble point, gas passes across the filter only by diffusion, but when the pressure is high enough to dislodge liquid from the pores, bulk flow begins and bubbles will be seen. The initial bubble test pressure determines the size (and location) of the largest pore, the open bubble-point pressure determines the mean pore size of the GDL. The latter can be affected by flow velocity as well as pressure. The theoretical relation between this transition pressure and the bubble-point pressure is:

$$D = \frac{4g\ \cos\theta}{P}$$

where P is the bubble-point pressure, g the surface tension of the liquid (72 dyn cm^{-1} for water), θ the liquid–solid contact angle and D is the diameter of the pore. Since no pores in the GDL are likely to be shaped like capillary tubes it is necessary to introduce a shape correction factor (0–1; it takes a value of 1 for a perfect cylindrical pore) into the formula. Since values of g and θ are constants for various GDL samples with identical PTFE content (30%), the formula can be simplified by introducing an empirical factor, K. Therefore,

$$D = \frac{K}{P}$$

where D is again the maximum average diameter of the pores in μm. It is a non-destructive test, thus it does not contaminate the GDL samples.

Catalyst coated membranes (CCM) with 5 cm^2 geometrically active area electrodes were fabricated by using 50 wt.% Pt on carbon catalyst (Tanaka TEC1050E) by a micro-spray method on Nafion-112 membrane. The catalyst loadings on both anode and cathode sides were about 0.5 mg Pt cm^{-2}. The GDLs and the CCM were not hot-pressed but assembled by just sandwiching inside the test cell (Greenlight G50 fuel cell system, Hydro-

genics, Vancouver, Canada). Gas sealing was carried out using silicone coated fabric materials (Performance Plastics, CF1007) and with a uniform torque of 40 lb in. [19]. Single cell fuel cell performance was assessed using Fuel Cell Technologies Test Station, at 70 °C with H_2/air under ambient pressure by galvanostatic polarization. The gas flow rates were fixed at 100 and 300 sccm for hydrogen and air, respectively. The steady state voltage values at were collected by holding the cell for 1 min at each current density values. The relative humidity of the reactant gases was maintained at 100% by controlling the humidity bottle temperatures.

3. Results and discussion

Fig. 1(a–c) shows the surface morphology of GDLs fabricated by using Vulcan XC-72R carbon, nano-chain Pureblack carbon and a mixture of Pureblack with nano-fibrous carbon as micro-porous layer, respectively. The SEM micrographs of the GDLs showed crack free micro-porous layer favoring uniform gas distribution. As seen from Fig. 1(b and c) unique nodular, somewhat coarse, growth like structure was observed for GDLs with nano-chain Pureblack carbon and Pureblack + nano-fibrous carbon based micro-porous layers. The surface of the structure has many peaks and valleys. Microscopic examination with a SEM was also done on the cross section of the gas diffusion layer. Examining the cross sections in Fig. 2 shows that the coating thickness ranges from 50 to 60 μm. In addition, the GDL cross section does not show any carbon bleed-through from the

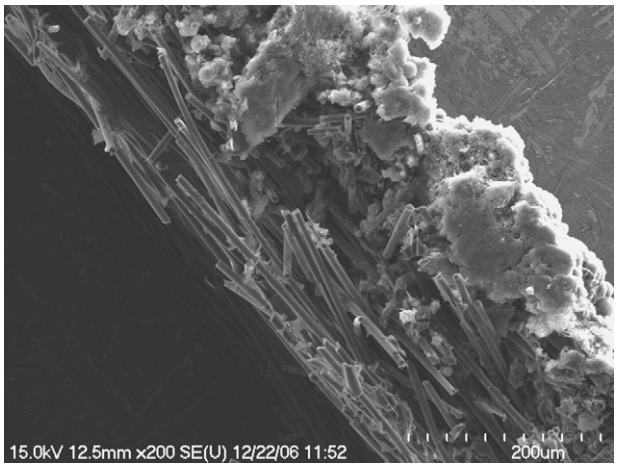

Fig. 2. Cross section of gas diffusion layer using Pureblack + nano-fibrous carbon based micro-porous layer by scanning electron microscope.

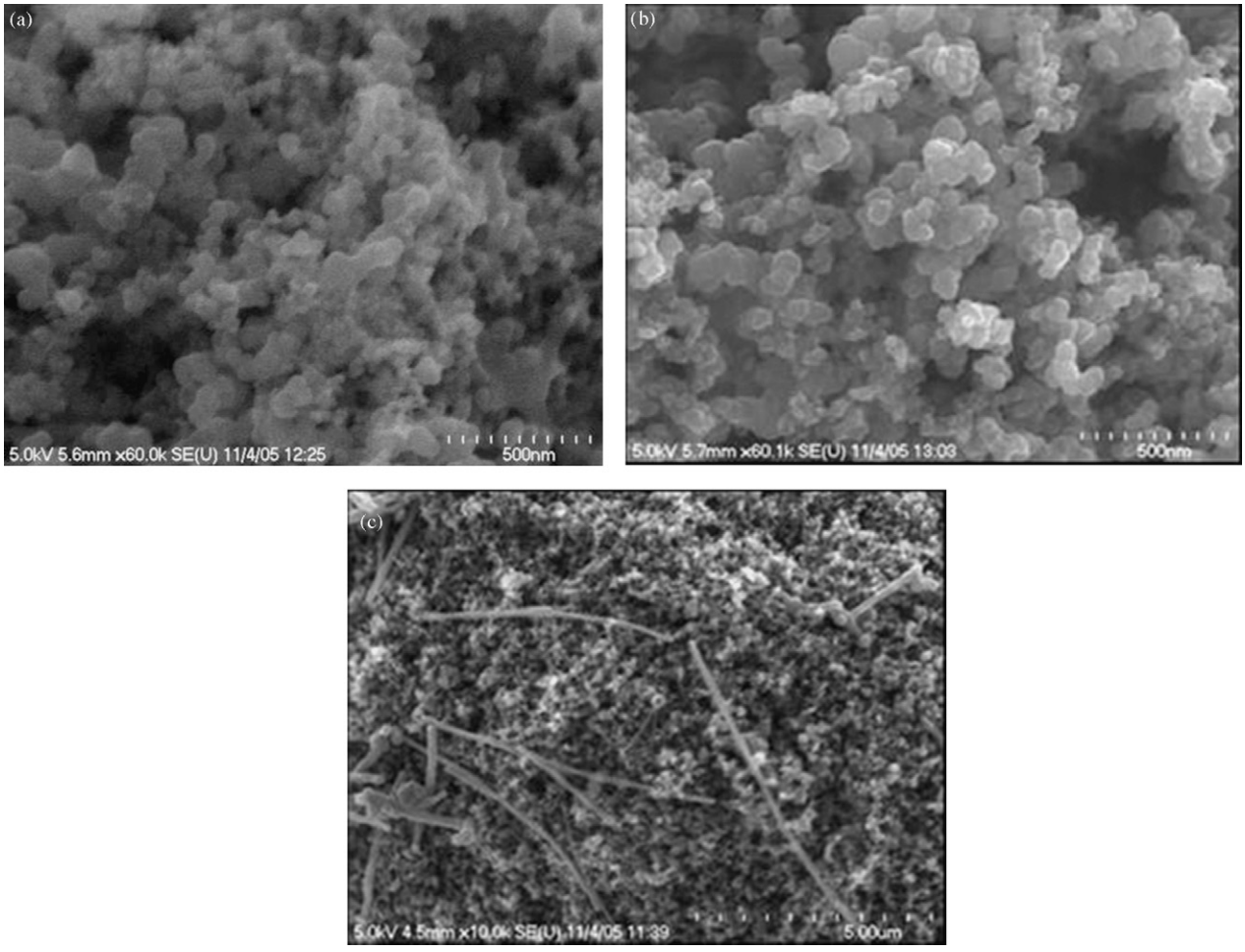

Fig. 1. Scanning electron micrographs of gas diffusion layer using (a) Vulcan XC-72R, (b) Pureblack nano-chain carbon and (c) Pureblack + nano-fibrous carbon based micro-porous layers.

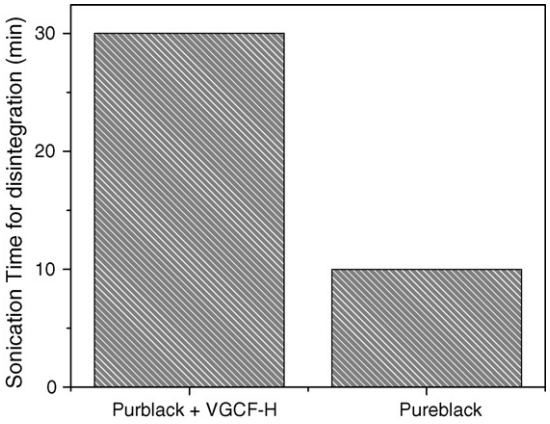

Fig. 3. Mechanical stability of gas diffusion layers from ultrasonication.

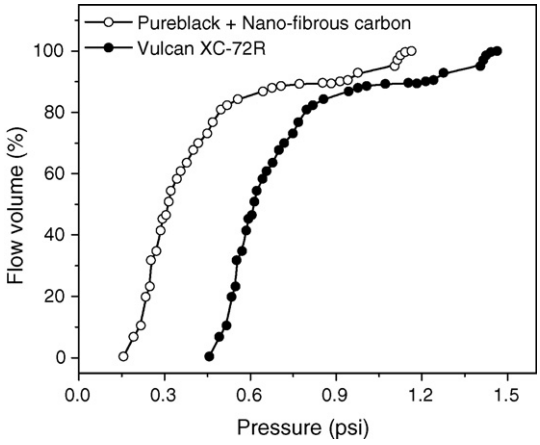

Fig. 4. Bubble-point pressure for Vulcan XC-72R and Pureblack + nano-fibrous carbon based GDLs at room temperature.

micro-porous layer to the uncoated side of the macro-porous carbon paper substrate.

The purpose of adding nano-fibrous carbon to Pureblack was to impart structural integrity to the micro-porous layer of the GDL. The structural robustness and the effectiveness of adhesion of the micro-porous layer to the macro-porous layer were attained by subjecting the GDLs to ultrasonication. One can conclude based on the disintegration time interval histograms shown in Fig. 3 that the GDL containing Pureblack + nano-fibrous carbon (VGCF-H) has higher mechanical stability (at least 3×) compared to that without nano-fibrous carbon. Hence, remaining tests including the fuel cell performance evaluations were carried out for GDLs with Pureblack + nano-fibrous carbon in the micro-porous layer.

The bubble-point pressure of GDLs with Vulcan XC-72R and Pureblack + nano-fibrous carbon based micro-porous layers are given in Fig. 4. GDL with Pureblack + nano-fibrous carbon show lower bubble-point pressure (0.16 psi as against 0.46 psi) due to the presence of larger pores compared to that with Vulcan, as the pore diameter is inversely proportional to bubble-point pressure given in the equation, $D = K/P$. The mean flow pore size calculated for Pureblack/nano-fibrous carbon based GDL is only about 24 μm. Therefore, it is expected that there will not be any additional restriction to gas flow for this micro-porous coating. Bubble-point pressure helps optimizing GDLs for various operating conditions.

The specific contributions to the surface energy for the GDL samples are calculated from the geometric mean of the γ_S^+ and γ_S^- numbers. The γ_S^+ and γ_S^- numbers were obtained from the specific free energy values of dichloromethane and ethyl acetate only. The acid (Ka) and base (Kb) numbers, based on the Gutmann concept, are listed in Table 1. These values were calculated using the specific free energy values of ethyl acetate, acetone, acetonitrile, and ethanol. For this study the entropic contribution to the free energy is assumed negligible, thus ΔH_s is approximated by ΔG_s. The Gutmann acid–base numbers in Table 1 (Ka and Kb) suggest an acidic surface for the Vulcan XC-72R based sample because the Ka (acid) number is much higher than the Kb (base) number. The base number (Kb) for the Vulcan XC-72R based GDL sample is measurable, so it does poses some basic character. For the GDLs with Pureblack + nano-fibrous carbon samples, the Gutmann acid and base numbers are similar, indicating an amphoteric nature for these two GDL samples. There are no differences in the Gutmann acid/base numbers for these samples. The Kb numbers are similar for all three samples, while the Ka number for the Vulcan XC-72R based GDL is much higher than that of the Pureblack + nano-fibrous carbon samples. The higher acidity for the Vulcan XC-72R based GDL suggests different surface groups are present for this sample.

According to the Good-van Oss acid–base theory, the γ_S^+ (acid, electron acceptor) and γ_S^- (base, electron donor) numbers are not directly comparable for the same sample. Therefore, it is not possible to arrive at a conclusion that a surface is more acidic or basic by simply comparing the γ_S^+ and γ_S^- values on the same sample. However, the γ_S^+ and γ_S^- numbers are comparable between samples (see Table 1). For instance, if sample X has a higher γ_S^- number than sample Y, then sample X is considered to be more basic than that of Y. Using the above guidelines, the acid numbers (γ_S^+) and base numbers (γ_S^-) for Pureblack + nano-fibrous carbon are much lower compared to the Vulcan XC-72R based GDL sample, indicating a less active surface.

The surface energy values of the GDLs based on Vulcan XC-72R as well as Pureblack + nano-fibrous carbon micro-porous

Table 1
IGC data for GDLs based on Vulcan XC-72R and Pureblack + nano-fibrous carbon micro-porous layers

Sample (micro-porous layer)	Gutmann acid and base values		Electron donor and acceptance numbers (mJ m^{-2})		Surface energy (mJ m^{-2})
	Ka	Kb	γ_S^+	γ_S^-	γ^T
Vulcan XC-72R	0.19	0.10	69.1	459.3	668.7
Pureblack + nano-fibrous carbon	0.11	0.09	24.4	120.9	160.6

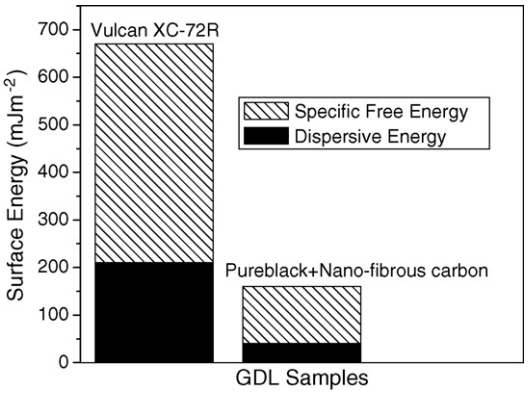

Fig. 5. Surface energy data as measured using inverse gas chromatograph for GDL samples with Vulcan XC-72R and Pureblack + nano-fibrous carbon based micro-porous layers.

layers are shown in Fig. 5. Even though, there is significant difference in both dispersive and specific surface energy values for GDLs with different micro-porous layers, surface energy values of GDLs estimated using Kruss Processor Tensiometer at CASE by Gurau et al. is much lower than what we have observed using IGC [16]. At this point it is not clear why there is a huge difference between the surface energy data reported here and the published data [16]. As seen from Fig. 5, the GDLs with Pureblack + nano-fibrous carbon show considerably much lower dispersive energy as well as specific free energies of desorption, compared to that with Vulcan XC-72R. In general, it is expected that the GDLs with higher surface energy values indicate a more active surface. Typically, this would correlate with the work of adhesion to micro-porous layer or interaction with product water during fuel cell operation.

Fig. 6 shows the pore size distribution for GDLs containing Vulcan XC-72R as well as Pureblack + nano-fibrous carbon micro-porous layers. Evidently, the GDL with Pureblack + nano-fibrous carbon micro-porous layer do not show pores with less than 0.1 μm. GDL with Pureblack + nano-fibrous carbon based micro-porous layer having larger pores coupled with lower surface energy is expected to perform very well at higher current density without flooding.

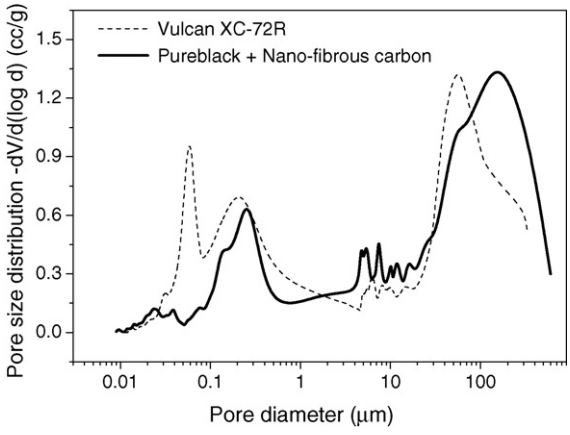

Fig. 6. Pore size distribution data as measured using Hg porosimetry for a GDL sample with Pureblack + nano-fibrous carbon based micro-porous layer.

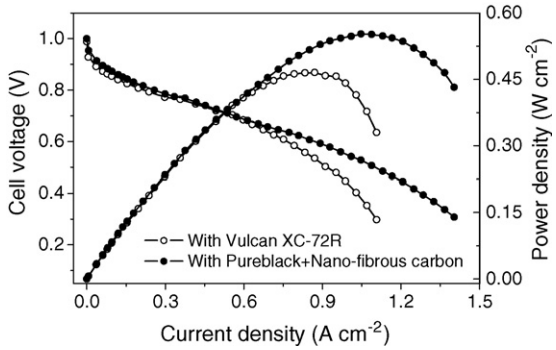

Fig. 7. Fuel cell performance of MEAs with gas diffusion layer using (a) Vulcan XC-72R and (b) Pureblack + nano-fibrous carbon based micro-porous layers, at 70 °C, H_2/air, 100% RH and ambient pressure.

Fuel cell performance of MEAs at 70 °C using hydrogen and air at ambient pressures for GDLs containing Vulcan XC-72R and Pureblack/nano-fibrous carbon based micro-porous layers are shown in Fig. 7. Power density of 0.55 W cm^{-2} with hydrogen/air at ambient pressure was obtained for MEA at 70 °C using GDLs with Pureblack/nano-fibers. The data presents excellent gas diffusion (mass transport) characteristics of the GDLs fabricated with carbon nano-fibers along with Pureblack nano-chain carbon. As expected nano-fibers along with Pureblack nano-chain carbon micro-porous layer based GDL with lower surface energy values and larger pores (>0.1 μm) show excellent mass transport characteristics. However, the long-term performance, oxidative (chemical and electrochemical) stability needs to be ascertained at various operating conditions [14]. It is also necessary to optimize the composition of Pureblack + nano-fibrous carbon in the micro-porous layer for further improving the mass transport characteristics of GDLs. The performance optimization would be carried by statistical factorial design.

4. Conclusion

A composite micro-porous layer using carbon nano-chain Pureblack + nano-fibrous carbon (VGCF-H) in the GDL for proton exchange membrane fuel cell was demonstrated for the first time. The GDL was characterized by physico-chemical as well as electrochemical methods. It is also shown that the mechanical robustness of the micro-porous layer was improved by the presence of fibrous nano-carbon. The ex situ characterization techniques such as gas permeability for bubble-point pressure and inverse gas chromatograph for surface energy were found to be excellent tools for characterizing and selecting GDLs for specific operating conditions of proton exchange membrane fuel cells with hydrogen/air at ambient pressure. There exists a clear qualitative relationship between the surface energy values and the fuel cell performance for GDLs. The membrane electrode assembly with nano-chain Pureblack + nano-fibrous carbon (VGCF-H) based GDLs show power density of as high as 0.55 W cm^{-2} at 70 °C using hydrogen/air, 100% RH and ambient pressure with Nafion-112 membrane.

Acknowledgements

Financial support from ASU is duly acknowledged. The authors thank John Wertz, Hollingsworth & Vose Company and Daniel Burnett, Surface Measurement Systems Inc. for permeability and surface energy measurements of the GDLs, respectively.

References

[1] M.V. Williams, E. Begg, L. Bonville, H.R. Kunz, J.M. Fenton, J. Electrochem. Soc. 151 (2004) A1173.
[2] M.V. Williams, Ph.D. Thesis, University of Connecticut, 2004.
[3] J. Mirzazadeh, E. Saievar-Iranizad, L. Nahavandi, J. Power Sources 131 (2004) 194.
[4] C. Lim, C.Y. Wang, Electrochim. Acta 49 (2004) 4149.
[5] G. Park, Y. Sohn, T. Yang, Y. Yoon, W. Lee, C. Kim, J. Power Sources 131 (2004) 182.
[6] J. Chen, T. Matsuura, M. Hori, J. Power Sources 131 (2004) 155.
[7] W.M. Yan, C.Y. Soong, F. Chen, H.S. Chu, J. Power Sources 125 (2004) 27.
[8] L.R. Jordan, A.K. Shukla, T. Behrsing, N.R. Avery, B.C. Muddle, M. Forsyth, J. Appl. Electrochem. 30 (2000) 641.
[9] J.R. Yu, Y. Yoshiskawa, T. Matsuura, M.N. Islam, M. Hori, Electrochem. Solid-State Lett. 8 (2005) A152.
[10] M. Neergat, A.K. Shukla, J. Power Sources 104 (2002) 289.
[11] R. Roshandela, B. Farhanieha, E. Saievar-Iranizad, Renewable Energy 30 (2005) 1557.
[12] I.E. Baranov, S.A. Grigoriev, D. Ylitalo, V.N. Fateev, I.I. Nikolaev, Int. J. Hydrogen Energy 31 (2006) 203.
[13] Y. Bultel, K. Wiezell, F. Jaouen, P. Ozil, G. Lindbergh, Electrochim. Acta 51 (2005) 474.
[14] C. Lee, W. Mérida, J. Power Sources 164 (2007) 141.
[15] V. Gurau, M.J. Bluemle, E.S. De Castro, Y. Tsou, T.A. Zawodzinski, J.A. Mann, J. Power Sources 165 (2007) 793.
[16] V. Gurau, M.J. Bluemle, E.S. De Castro, Y. Tsou, J.A. Mann, T.A. Zawodzinski, J. Power Sources 160 (2006) 1156.
[17] X. Wang, H. Zhang, J. Zhang, H. Xu, Z.Q. Tian, J. Chen, H.X. Zhong, Y.M. Liang, B. Yi, Electrochim. Acta 51 (2006) 4909.
[18] X. Wang, H. Zhang, J. Zhang, H. Xu, X. Zhu, J. Chen, B. Yi, J. Power Sources 162 (2006) 474.
[19] A.M. Kannan, A. Menghal, I. Barsukov, Electrochem. Commun. 8 (2006) 887.
[20] A.M. Kannan, V. Veedu, L. Munukutla, M.N. Ghasemi-Nejhad, Electrochem. Solid State Lett. 10 (2007) B47.
[21] G. Garnier, W.G. Glasser, Polym. Eng. Sci. 36 (1996) 885.
[22] F.J. Lopez-Garzon, M. Pyda, M. Domingo-Garcia, Langmuir 9 (1993) 531.
[23] H. Darmstadt, C. Roy, H. Cormier, Rubber Chem. Technol. 70 (1997) 759.
[24] A.K. Jena, K.M. Gupta, J. Power Sources 80 (1999) 46.